Insight and prediction of spudcan elastic stiffness profile in stiff-over-soft clays

Wang, Xiu Zhe; Wang, Xin Tong; Wang, Zhen; Liu, Fei; Gao, Qiang Qiang; Yi, Jiang Tao

DOI
10.1016/j.marstruc.2025.103840

Publication date
2025

Document Version
Final published version

Published in
Marine Structures

Marine Structures 103 (2025) 103840

Contents lists available at ScienceDirect

Marine Structures

journal homepage: www.elsevier.com/locate/marstruc

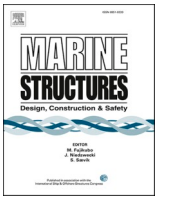

Insight and prediction of spudcan elastic stiffness profile in stiff-over-soft clays

Xiu Zhe Wang [a,b], Xin Tong Wang [c], Zhen Wang [b,d], Fei Liu [b,e], Qiang Qiang Gao [f], Jiang Tao Yi [b,*]

[a] Faculty of Civil Engineering and Geoscience, Delft University of Technology, Stevinweg 1, Delft 2628CN, Netherlands
[b] School of Civil Engineering, Chongqing University, Shabei Street 83, Chongqing 400045, China
[c] Nanjing Hydraulic Research Institute, Hujuguan Road 34, Nanjing 210024, China
[d] Changjiang River Scientific Research Institute, Chongqing Branch, Gangcheng East Road 2, Chongqing 400026, China
[e] School of Civil and Transportation Engineering, Henan University of Urban Construction, Longxiang Avenue, Pingdingshan 467000, China
[f] School of Mines, China University of Mining and Technology, Daxue Road 1, Xuzhou 221116, China

ARTICLE INFO

Keywords:
Elastic stiffness
Spudcan
Punch-through failure trend
Numerical modeling
Soil stratification
Layered clays

ABSTRACT

The elastic stiffness of spudcan foundations in stiff-over-soft clays exhibits changes similar to "punch-through" failure, creating significant uncertainty for jack-up platform operations. This study conducted a three-dimensional small-strain finite element analysis on this specific topic to discretely simulate the spudcan elastic stiffness profile in stiff-over-soft clay. The influence of the soil surface, layered interface, and their coupling effects were isolated and separately evaluated, and a simple semi-theoretical framework for the influence zone was proposed. The key parameters of layered soil (thickness ratio, shear modulus ratio, soil heterogeneity coefficient, and backflow) affecting the influence mechanism of spudcan elastic stiffness were evaluated and analyzed. It was found that the effects of the soil surface and layered interface competed with each other. The vertical deformation mechanism of the spudcan reduces the "punch-through" failure risk of elastic stiffness by transferring more of the soil deformation to the bottom soft clay layer. Based on the findings from the parameter study, a simplified profile is proposed to predict the variation of the spudcan elastic stiffness. The proposed prediction method provides a comprehensive view of elastic stiffness in stiff-over-soft clay for offshore in-site assessment.

1. Introduction

Spudcan, which serves as the foundation for mobile jack-up platforms, is widely used in drilling, exploration, and site investigation in the offshore oil and gas industry [23], and its operational and mechanical properties are closely related to the performance and safety of the platform [7,15]. The elastic load-displacement response or elastic behavior quantified by the elastic stiffness of the foundations under small strain conditions is a crucial aspect for the safe design of spudcan [1,7,15,20,21]. Accurate measurement of elastic stiffness is essential for predicting structural deformation and is applied directly as a boundary condition in the overall analysis of platform structures [8]. The load-displacement response and dynamic properties, such as inherent frequency and natural period, of platform structures are affected by elastic stiffness [10].

* Corresponding author.
E-mail addresses: X.Z.Wang@tudelft.nl (X.Z. Wang), yijt@foxmail.com (J.T. Yi).

https://doi.org/10.1016/j.marstruc.2025.103840
Received 24 February 2025; Received in revised form 15 April 2025; Accepted 4 May 2025
Available online 9 May 2025

Nomenclature

D	Spudcan diameter
E	Young's modulus
G	Shear modulus
G_{b0}	Shear modulus of bottom stiff clay
G_{bs}	Shear modulus of the bottom soft clay in the layered interface
G_t	Shear modulus of top stiff clay
G_{bs}/G_t	Shear modulus ratio
I_r	Rigidity index
k	Gradient of strength with depth
kD/s_{ubs}	Soil heterogeneity
K_V, K_H, and K_M	Elastic stiffness coefficients for vertical, horizontal and moment
R	Spudcan radius
s_u	Undrained shear strength
s_{ub0}	undrained shear strength of bottom stiff clay
s_{ubs}	undrained shear strength of the bottom soft clay in the layered interface
s_{ubt}	undrained shear strength of top stiff clay
t	Thickness of top soft clay
t/D	Thickness ratio of top soft clay
V, H and M	Vertical, horizontal and moment load
w	Embedment depth
$\overline{w}$	Normalized embedment depth
ν	Poisson' ratio
ε_1, ε_2, ε_3, ε_4, and ε_5	Fitting parameter
δ	Increment
ξ	Shear strain
ξ_{max}	Maximum value of ξ
w, u and φ	Vertical, horizontal and moment displacement

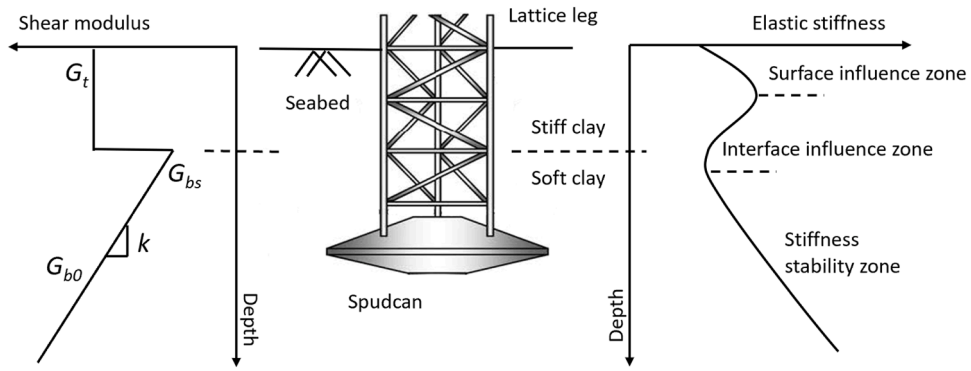

Fig. 1. Elastic stiffness profile of a spudcan operating in stiff overlying soft clays.

Due to the complex influence of geological structures and sediment transport, the clayey seabed commonly found in the operational areas of jack-up platforms sometimes may form a stiff layer at the soil surface [15] (see Fig. 1). The mechanical properties of clays vary significantly with depth [5]. This causes the spudcan elastic stiffness to change significantly with depth, especially when the spudcan is installed at the soil layered interface (which is analogous to the "punch-through" failure of spudcan penetration resistance [26]) (see Fig. 1). Underestimating the spudcan elastic stiffness may result in overestimating stresses in critical components during structural analysis, such as the hull-leg joint. Conversely, overestimating the spudcan elastic stiffness may lead to inaccuracies in predicting the load paths within the structure, especially in components that have significant dynamic effects [2,3]. Therefore, the seabed geological environment of stiff-over-soft clay introduces significant uncertainty into the site-specific assessment of jack-up platforms.

To date, the significant effect of stiff-over-soft clay on the working/mechanical behavior of spudcan has been widely reported but has mainly focused on predicting and evaluating the potential risk of spudcan "punch-through" failure [13,14,26]. The understanding of spudcan elastic behavior under different soil properties (i.e., heterogeneity [24,25], spatial variability [20]) and behaviors (i.e., installation [17], consolidation [21]) has also been further improved but has ignored the scenario of soil stratification. At present,

Table 1
Summary of SSFE analyses performed.

Analysis	t/D	G_{bs}/G_t	kD/s_{ubs}	Geometry	Note
Group I	2	5	0	Circular plate	Validation
	0	∞	1	Spudcan	Validation
Group II	100	0.2	0	Spudcan	Effect of layered interface
Group III	0	∞	0	Spudcan	Effect of surface boundary
Group IV	2	0.5	0, 1	Spudcan	Coupling effect
Group V	0.5 - 2	0.5	1	Spudcan	Parametric study
Group VI	1	0.1 – 0.9	1	Spudcan	Parametric study
Group VII	1	0.5	0 - 3	Spudcan	Parametric study
Group VIII	0.5	1	1	Spudcan	No backflow, Complete backflow
Group IX	0.25–2	0.1–0.9	0–3	Spudcan	Prediction method

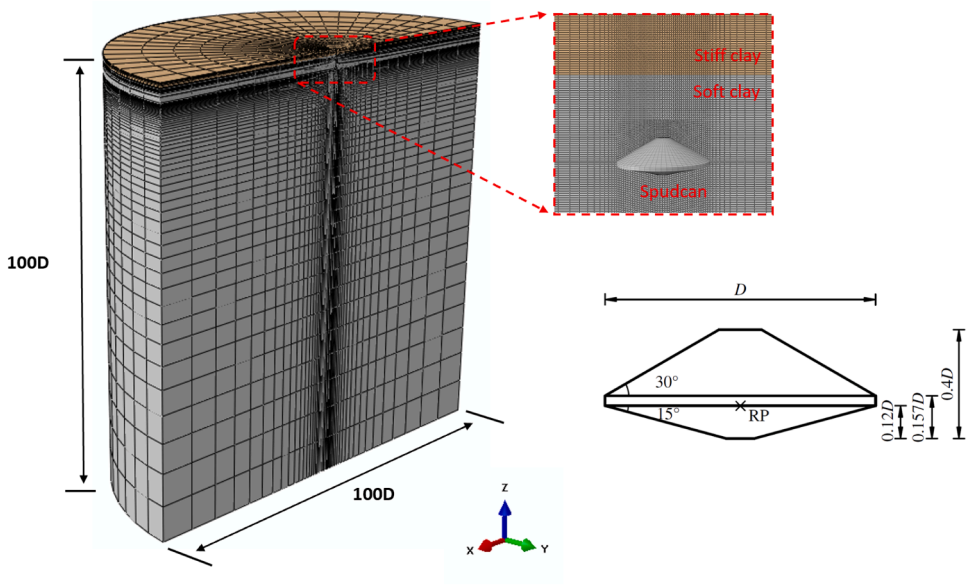

Fig. 2. Finite element models for the SSFE analysis and spudcan shape.

there exists a significant knowledge gap in studying the spudcan elastic behavior in stiff-over-soft clay, although ISO [15] points out the necessity of carefully evaluating the spudcan elastic stiffness in layered soil. Wang et al. [22] have also confirmed preliminarily that the influence of soil stratification characteristics on the elastic stiffness of circular foundations in clay-over-sand is significant.

Given this, the elastic stiffness and deformation mechanism of spudcan foundations in stiff-over-soft clay are studied using three-dimensional small-strain finite element (SSFE) analysis. The corresponding profile of changes in elastic stiffness of the spudcan at different depth positions in stiff-over-soft clay is discretely simulated. The specific study objectives include: (a) to investigate the influence mechanisms of the soil surface boundary and soil layer interface; (b) to analyze the variation in elastic stiffness and the corresponding mechanisms under different soil stratification conditions; and (c) to fill the gaps in the database and prediction methods in current studies of spudcan elastic stiffness, providing insights for a more accurate in-situ assessment.

2. Numerical analysis

2.1. Soil behavior and properties

In this study, the stiff-over-soft clay is modeled as a weightless, isotropic elastic material and adopt the Tresca constitutive model to facilitate accurate analysis of the elastic behavior of the spudcan. The relationship between the load increments (δV, δH and δM) and elastic displacement increments (δw, δu and $\delta \varphi$)of the spudcan in stiff-over-soft clay is defined by the following equation:

$$\begin{Bmatrix} \delta V/GR \\ \delta H/GR \\ \delta M/GR^3 \end{Bmatrix} = \begin{bmatrix} K_V & 0 & 0 \\ 0 & K_H & 0 \\ 0 & 0 & K_M \end{bmatrix} \begin{Bmatrix} \delta w \\ \delta u \\ \delta \varphi \end{Bmatrix} \tag{1}$$

Where K_V, K_H and K_M are the vertical, horizontal and moment elastic stiffness coefficients of the spudcan; R is the spudcan radius; G is

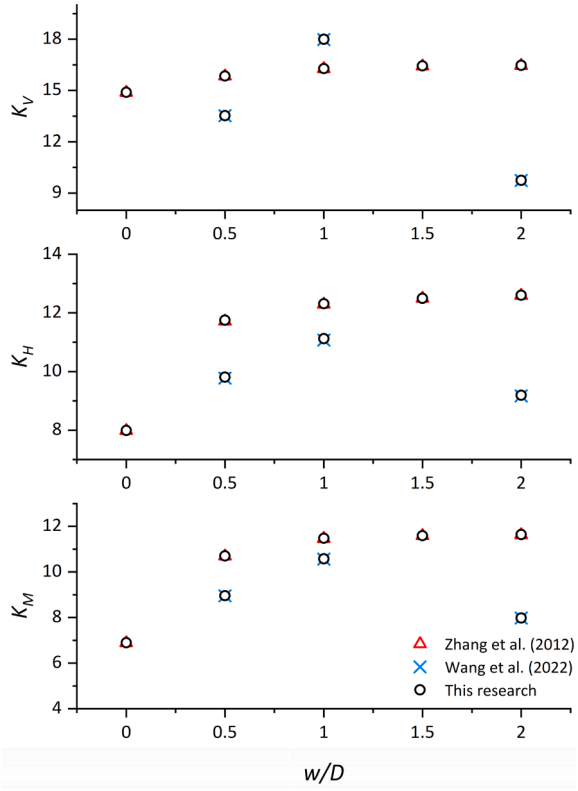

Fig. 3. Validation of the numerical model using existing solutions.

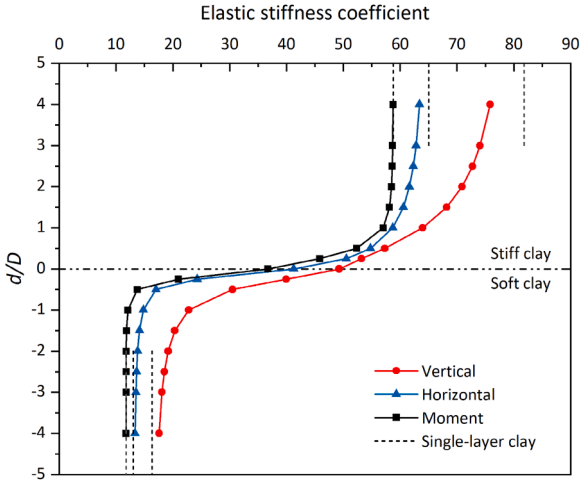

Fig. 4. Elastic stiffness coefficients of spudcan foundations in stiff-over-soft clay with approximately infinite embedment depth.

the initial shear modulus (or undisturbed shear modulus) chosen for normalizing the elastic stiffness.

According to the actual range of stiff-over-soft clay properties reported in the literature [13,14], the typical property parameters of stiff-over-soft clay in this study are as follows: undrained shear strength of top stiff clay $s_{ut} = 30$ kPa; undrained shear strength of the bottom soft clay $s_{ub0} = s_{ubs} + k(z - t)$, where the undrained shear strength of the bottom soft clay in the layered interface $s_{ubs} = 15$ kPa, the strength gradient of the bottom soft clay $k = 1.25$ kPa/m, and the thickness of the top stiff clay $t = 1D$.

In addition, since the rigidity index of clay $I_r = G/s_u$ has no significant influence on the spudcan elastic stiffness [20,24], this study set I_r at 168.7 to keep $E/s_u = 500$ consistent with previous studies [4,17,20,25]. The Poisson's ratio of soil ν is 0.49 to simulate no volume change in saturated clay under undrained conditions and also to ensure the stability of the numerical simulation [18–20]. For ease of comparison, the dimensionless results of the parameter combinations discussed in this study are presented in Table 1, where G_t

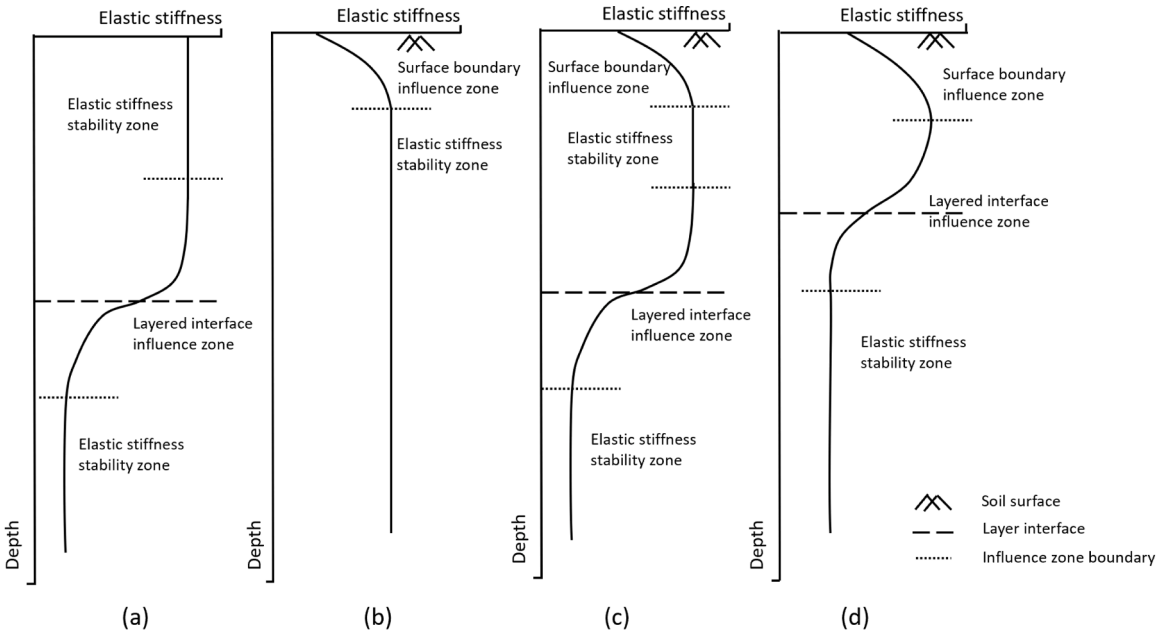

Fig. 5. Elastic stiffness curves and influence zone distribution under different soil boundaries and layered interfaces (a) Layered soil profiles with infinite depths, (b) Single-layer soil profile with infinite depth, (c) Ideal layered soil profile, and (d) Realistic layered soil profile.

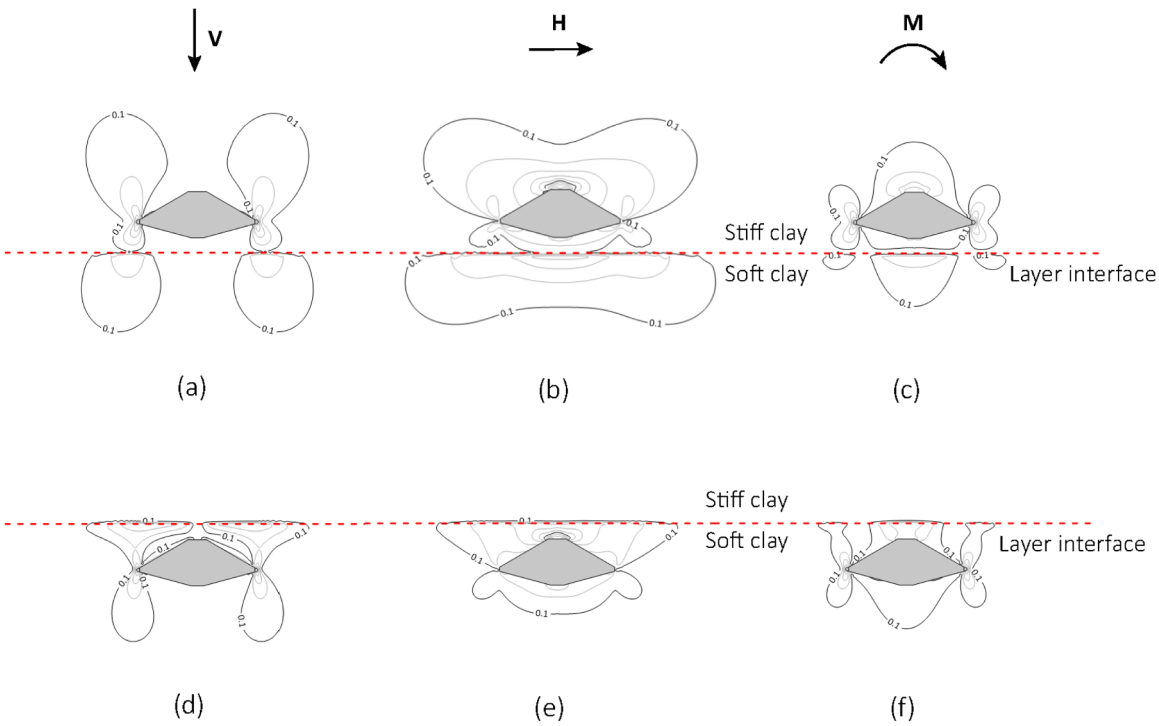

Fig. 6. Shear strain distribution of spudcan foundation in stiff-over-soft clay with approximately infinite embedment depth.

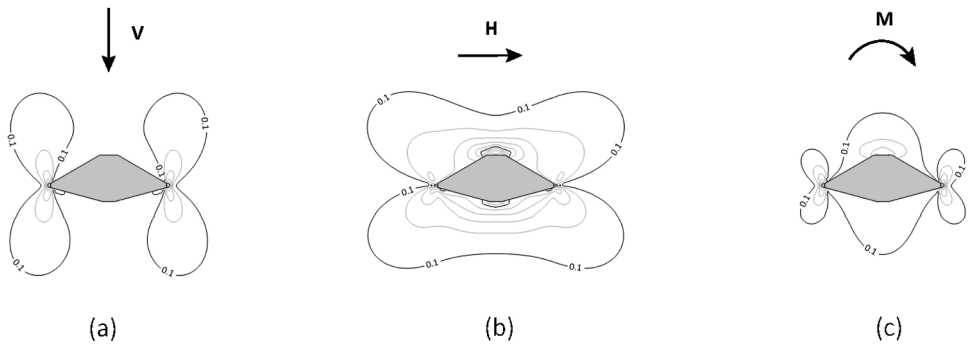

Fig. 7. Shear strain distribution of spudcan foundation in single-layer clay with approximately infinite embedment depth.

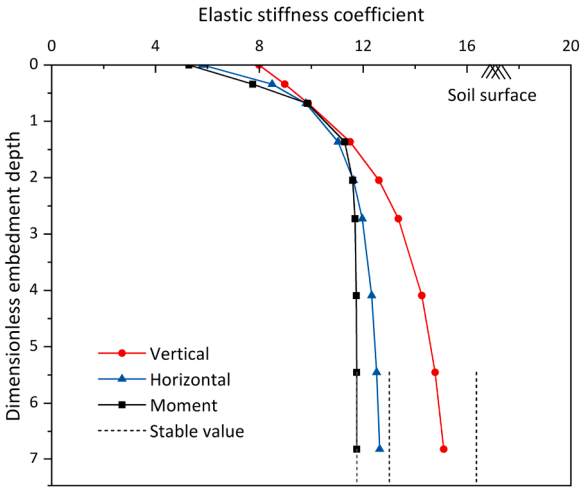

Fig. 8. Elastic stiffness coefficients of spudcan foundations in single-layer clay.

is the initial (or undisturbed) shear modulus of top stiff clay. These parameter combinations cover the practical range for layered clay [13,14,26].

2.2. Finite element model

The three-dimensional small-strain finite element (SSFE) analysis was conducted using the commercial finite element software ABAQUS [6]. Following previous solutions [20,22,25], the spudcan foundation is embedded in undisturbed or conditioned soil based on the "wished-in-place" assumption. The spudcan was simulated at a series of discrete embedment depths using the SSFE technique, covering the range from the soil surface through the upper stiff clay layer and across the interface into the underlying soft clay. The embedment depth was varied in intervals of D/12, where D is the spudcan diameter, to capture the variation in elastic stiffness within the stiff-over-soft clay profile. It is worth noting that although the "wished-in-place" assumption ignores the effects of remodeling and softening of the soil due to the spudcan penetration, which in turn leads to an overestimation of the elastic stiffness results, it can isolate and separately evaluate the effects of the soil surface and layered interface, which is more beneficial for understanding the elastic behavior of the spudcan in layered soil.

The geometry of the spudcan model is shown in Fig. 2, which was set as a rigid body, and the displacement control analysis was performed by applying the specified displacement at the reference point (RP). Due to the symmetry of the elastic stiffness problem of the spudcan in layered soil, a semi-cylindrical soil model with both a diameter and height of 100D was adopted to improve computational efficiency and avoid potential boundary effects [21,25]. The soil model was discretized into an 8-node Lagrangian reduced integration element (C3D8R) with a finer mesh near the spudcan model. After a mesh sensitivity analysis, it was determined that the minimum mesh size that ensured convergence of the computational results was 0.025D. The normal displacements of the soil model were constrained at the vertical slice face, the outer face, and the bottom face. The spudcan-soil contact interface was assumed to be fully rough and bonded to reasonably simulate the interface adhesion/bonding behavior due to the suction underneath the spudcan base [9] and the restraint of the upper backflow soil [12], thereby improving computational efficiency and convergence [20,21].

It is worth mentioning that the elastic stiffness coefficients in the dimensionless elastic stiffness matrix (Eq. (1)) were obtained from

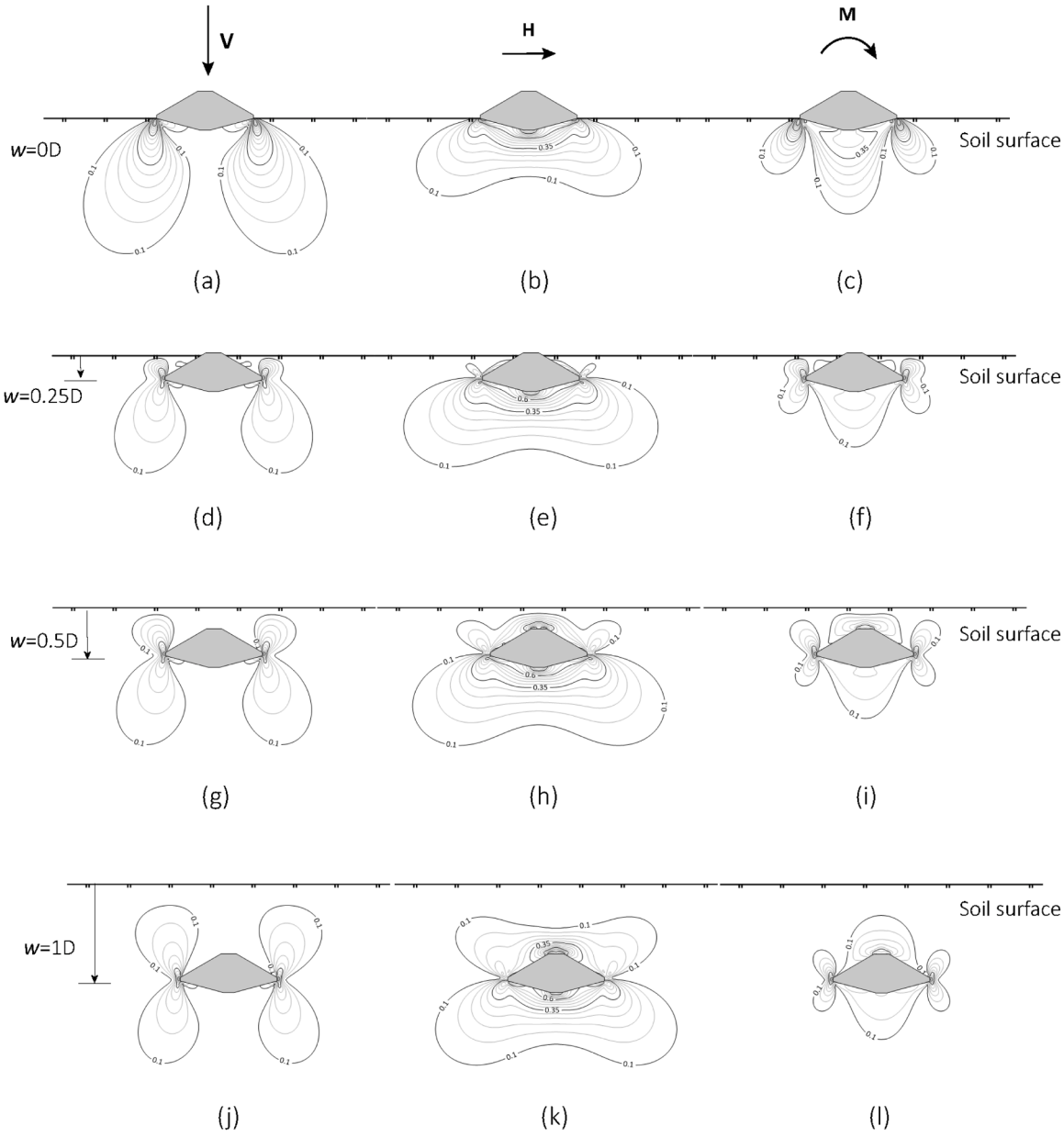

Fig. 9. Shear strain distribution of spudcan foundations in single-layer clay with different embedment depths.

displacement control tests (i.e., "probe" tests). Since the soil was modeled as an isotropic elastic material, a small initial displacement control test (e.g., 0.0001 m) was not required to capture the elastic characteristics of the initial load-displacement response. In this study, the initial velocities applied were 0.01 m/s or 0.01 rad/s.

3. Validation

So far, there is no theoretical solution for the elastic stiffness of spudcan, nor are there any field or experimental measurements. In fact, considering that the mechanical behavior of soils in practical engineering is always a combination of elasticity and plasticity, it is practically infeasible to accurately measure the elastic stiffness in a field or experimental environment. Therefore, this section verifies the finite element model by comparing the numerical solution of a circular plate foundation in clay-over-sand with the numerical solution of a spudcan foundation in a single-layer clay (Group I, Table 1). It can be seen from Fig. 3 that the elastic stiffness coefficients obtained under different soil stratification types and foundation types are very close to the known solutions, which is sufficient to demonstrate the validity of the finite element model. The same model boundaries and discretization methods have been validated for

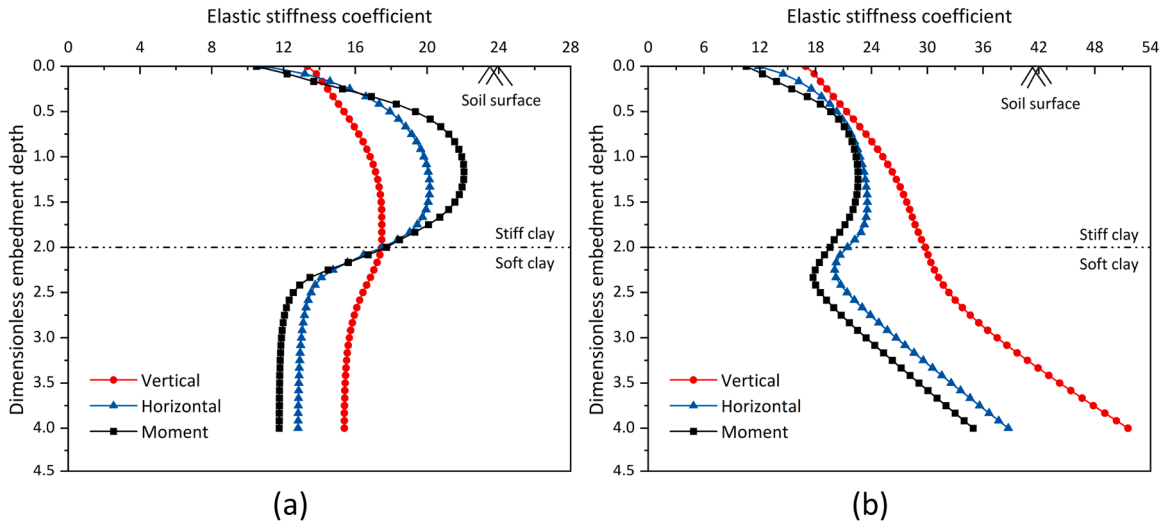

Fig. 10. Elastic stiffness coefficients of spudcan foundations in stiff-over-soft clay (a) bottom soft soil with $kD/s_{ubs} = 0$, (b) bottom soft soil with $kD/s_{ubs} > 0$.

elastic stiffness problems in other complex scenarios [20,21].

4. Results and discussion

4.1. Typical effects of soil stratification

4.1.1. Effect of layered interface

In order to isolate and individually evaluate the effect of the soil layered interface on the spudcan elastic stiffness, the spudcan is embedded at a depth of 100D (approximate infinite embedment depth) in this section (i.e., the distance of the spudcan from both the top and bottom boundaries of the soil model is 100D, and the soil model diameter remains unchanged at 100D), in order to remove the constraint effect of the soil surface boundary on the spudcan. In addition, the soil heterogeneity coefficient of the bottom clay layer $kD/s_{ubs} = 0$ to avoid the coupling effect of the strength gradient of the bottom soft clay and the shear modulus ratio $G_{bs}/G_t = 0.2$ (Group II, Table 1).

Fig. 4 shows the change of spudcan elastic stiffness in a stiff-over-soft clay at an approximately infinite depth, where d is the distance between the spudcan reference point and the soil layered interface. In order to compare and display the changes of elastic stiffness in three directions, normalization treatment was performed for the elastic stiffness using the spudcan radius R (see Eq. (1)). It is worth mentioning that, since the elastic stiffness coefficient value is closely related to the value of shear modulus G (see Eq. (1)). To show the influence of the interface on elastic stiffness, a constant G is used to dimensionless the elastic stiffness to avoid confusion, i.e., the shear modulus of the bottom soil clay at the layered interface G_{bs}, same below.

As shown in Fig. 4, before sensing the influence of soil stratification or the soil layered interface, or after leaving the influence of the layered interface, the elastic stiffness coefficient of the spudcan converges to the result of single-layer clay with the same stiffness level, indicating that the spudcan is in a stability zone (see Fig. 5(a)). When the spudcan gradually approaches the top stiff clay and crosses the layered interface into the bottom soft clay, the elastic stiffness coefficient of the spudcan gradually decreases after sensing the influence of the layered interface. At this time, the spudcan is in the influence zone of the layered interface (see Fig. 5(a)), which may be attributed to the difference in energy consumption of the spudcan foundation in the two clay layers.

Fig. 6 shows the shear strain distribution of the spudcan foundation in stiff-over-soft clay to demonstrate the variation and mechanistic of soil deformation when spudcan moves under load. Note that the shear strain ξ is normalized by ξ/ξ_{max} to uniformly quantify the shear strain distribution in three directions, where ξ_{max} is the maximum value of ξ in the soil domain.

When the spudcan is in the top stiff clay, the energy consumed for the soil to undergo the same degree of deformation while the spudcan moves under load is higher than that in the bottom soft clay. Therefore, without sensing the influence of the layered interface, the elastic stiffness in the top stiff clay is greater. After sensing the influence of the layered interface, the soil deformation spreads into the bottom soft clay (i.e., isolated deformation zones are formed in the soft clay, as shown in Figs. 6 and 7), similar to the isolated deformation zones in highly spatially variable soils described by Wang et al. [20], both due to significant differences in soil strength. This, to some extent, reduces the difficulty of soil deformation, thereby lowering the energy consumed and resulting in a decrease in elastic stiffness. After the spudcan enters the bottom soft clay, the top stiff clay layer provides a certain degree of isolation, causing the soil deformation to be mainly concentrated in the bottom soft clay. This further reduces energy consumption and makes the elastic stiffness in the soft clay significantly lower than that in the stiff clay.

It is worth noting that the spudcan elastic stiffness is much less likely to stabilize in stiff clay, i.e., the distance of the spudcan from

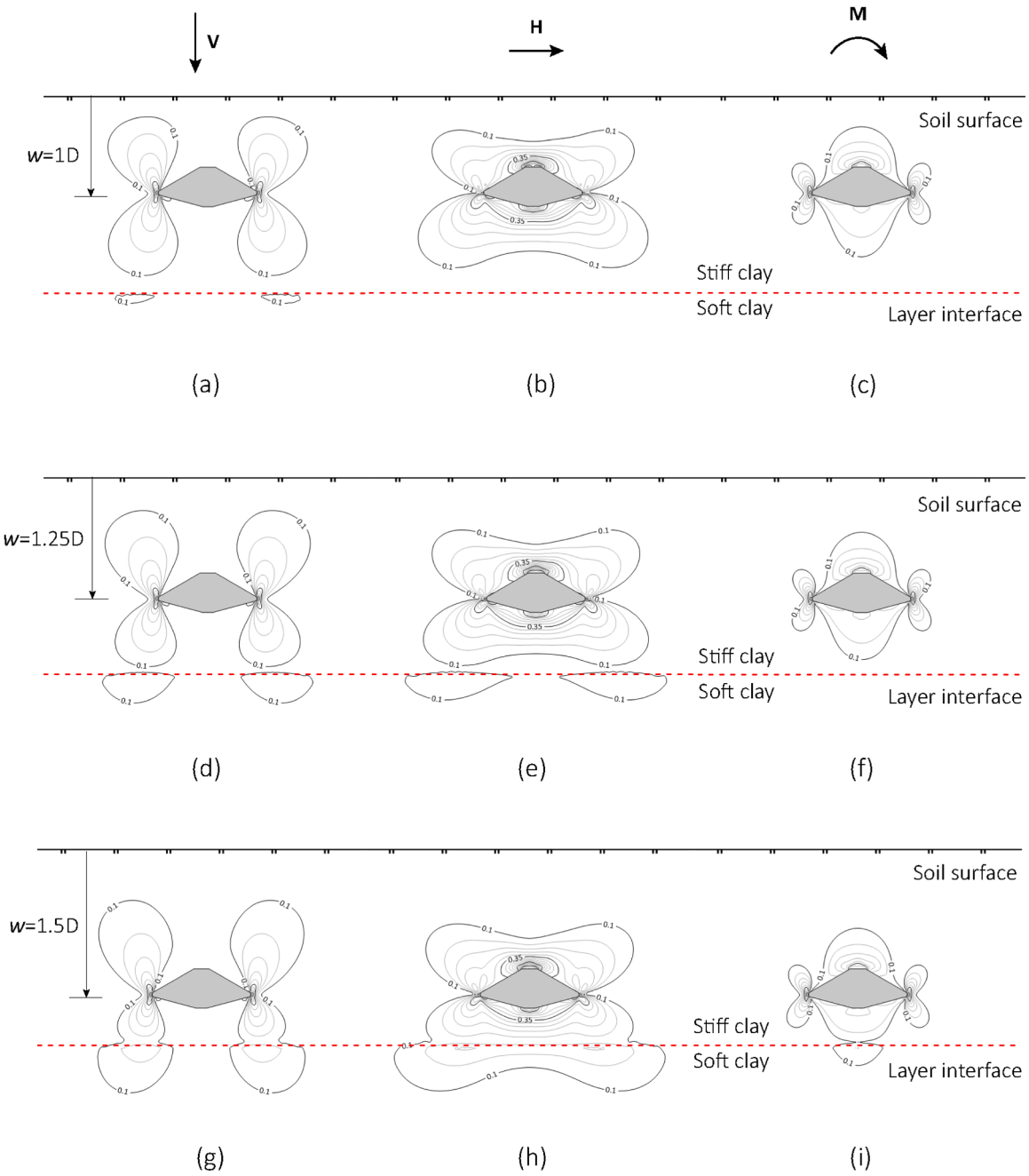

Fig. 11. Shear strain distribution of spudcan foundations in stiff-over-soft clay with different embedment depths.

the layered interface is greater when the elastic stiffness coefficient converges to a certain value (see Fig. 4). This may be because soil deformation is more likely to develop in soft clays; that is, the deformation mechanisms are more widely distributed in the soft clay (see Fig. 6), making it easier for the spudcan to sense the influence of the layered interface as it gradually approaches the soft clay from the stiff clay. When the spudcan is in soft clay, the isolation effect of the stiff clay reduces the extent of the influence of the layered interface on the spudcan.

Further observation of Fig. 4 shows that vertical, horizontal, and moment elastic stiffness exhibit different sensitivities to soil stratification and the soil layered interface. As the spudcan gradually approaches the layered interface from the top stiff clay, the change gradient of moment elastic stiffness is the largest, and the distance from the soil layer interface is the smallest when the change occurs. In contrast, the change gradient of vertical elastic stiffness is the smallest, and the distance from the soil layer interface is the largest when the change occurs. Additionally, the moment elastic stiffness converges to that of the single-layer clay soon after the

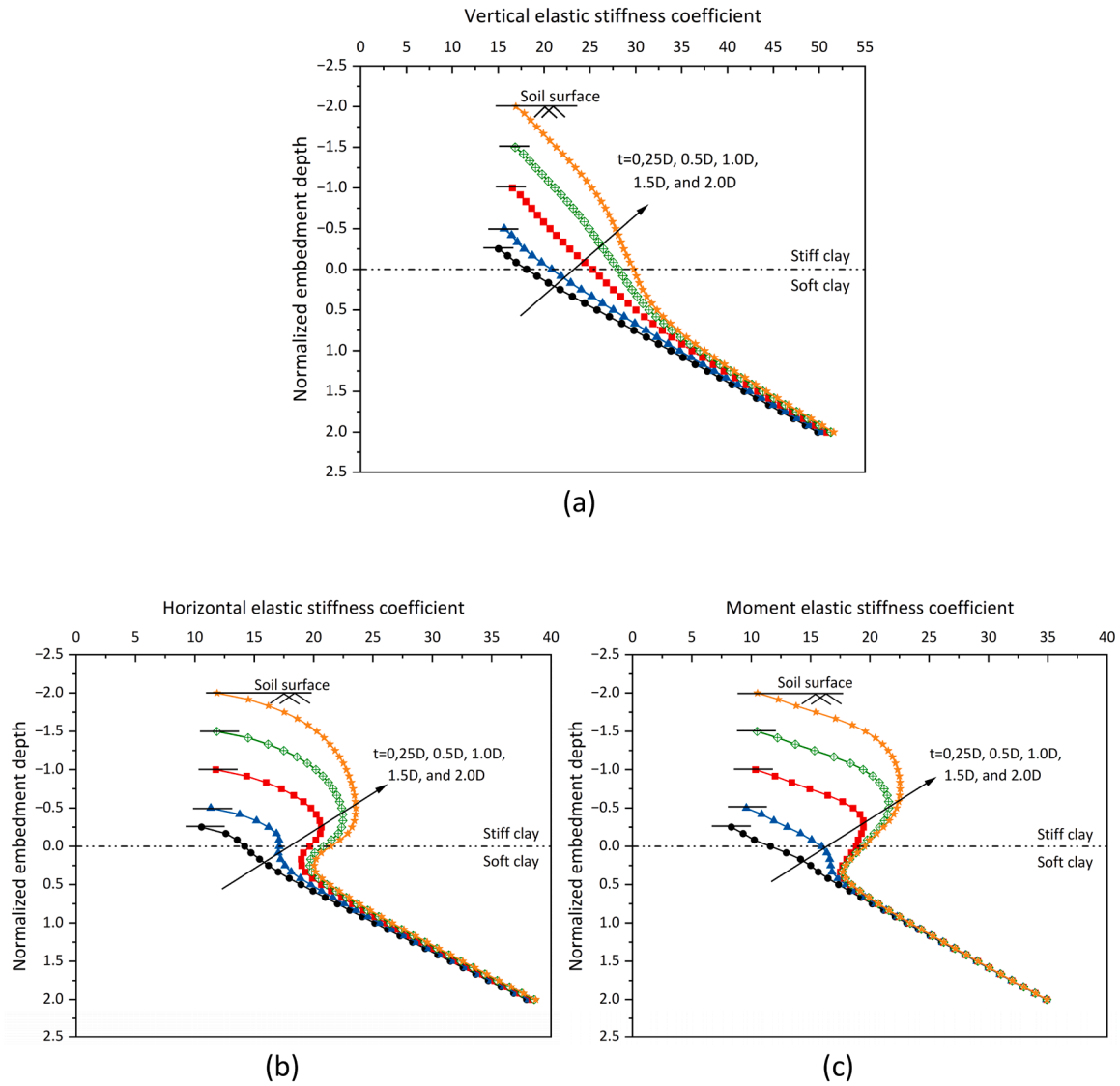

Fig. 12. Elastic stiffness coefficients of spudcan foundations in stiff-over-soft clay with different thickness ratios t/D.

spudcan crosses into the top stiff clay. At the same time, the vertical elastic stiffness still differs from the result of single-layer clay when the spudcan is a certain depth from the top stiff clay. This difference in spudcan elastic stiffness in layered soil may be attributed to the wider distribution of vertical deformation mechanisms in the depth direction (see Fig. 6) and the greater ease of sensing strength differences between layered interfaces.

4.1.2. Effect of surface boundary

The constrain effect of the soil surface boundary on the spudcan elastic stiffness has been emphasized many times in previous studies [17,20,21,25], but the mechanism of its influence has not been elucidated. In this section, the influence mechanism of the soil surface boundary is analyzed, and it is assumed that the spudcan enters the top stiff soil from the soil surface but has not yet sensed the soil layered interface and is only influenced by the soil surface boundary. Thickness ratio of the top stiff clay $t/D = 0$; $kD/s_{ubs} = 0$ to avoid the coupling effect of the strength gradient in the bottom soft clay (group III, Table 1).

As shown in Fig. 8, the elastic stiffness coefficient of the spudcan gradually increases as it enters the soil from the surface (i.e., gradually moving away from the soil surface boundary). After leaving the influence zone of the soil surface boundary, the spudcan elastic stiffness gradually tends to stabilize and eventually converges to the elastic stiffness result in the stability zone, at which point the spudcan enters the stability zone (see Fig. 5(b)). This behavior is related to the soil surface boundary reducing the energy consumption associated with soil deformation.

As shown in Fig. 9, the soil surface boundary acts like a stiff clay layer with infinite strength, isolating the development of shear strain and reducing the energy consumed by soil deformation. As the embedment depth of the spudcan increases, the distribution range

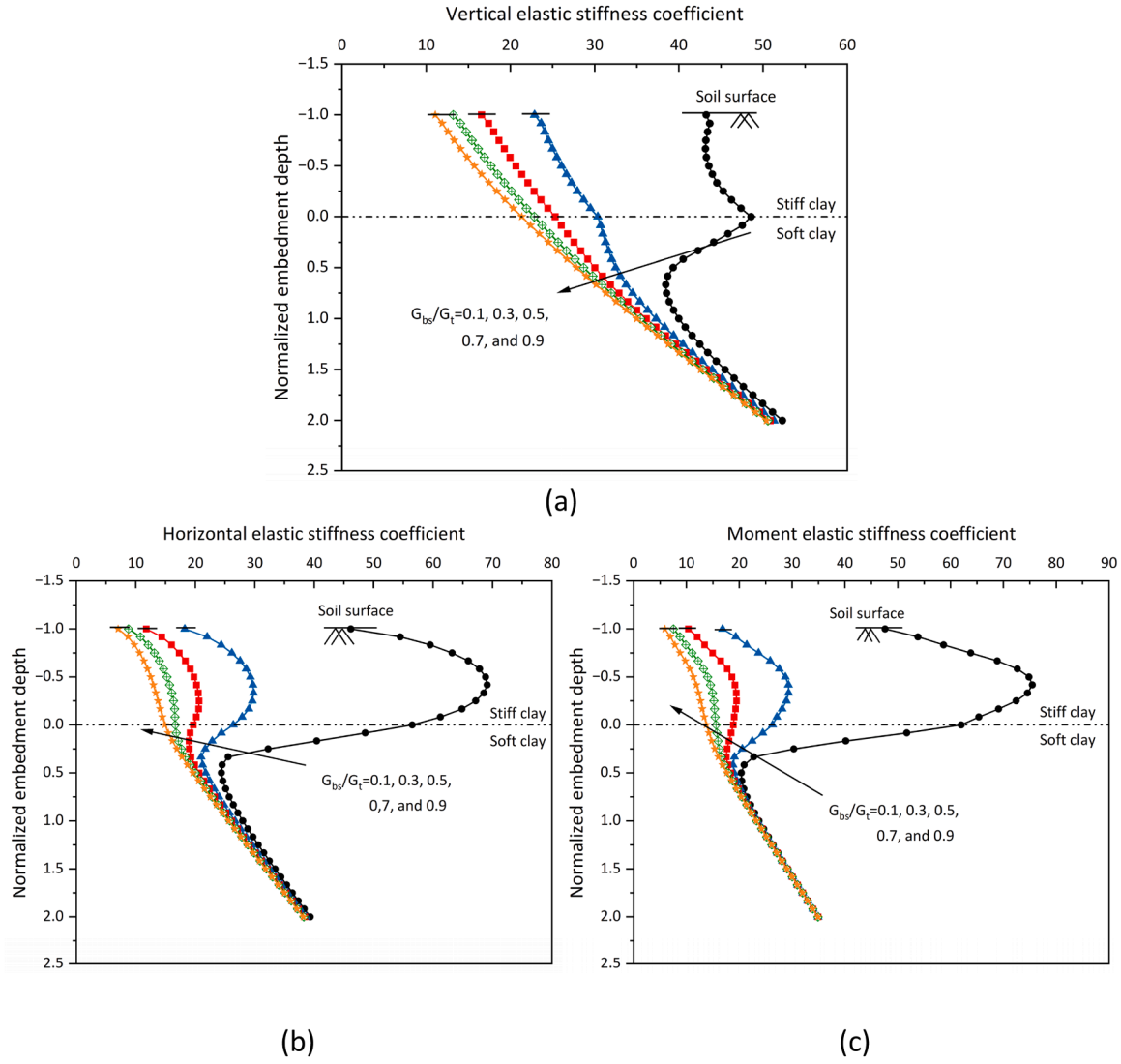

Fig. 13. Elastic stiffness coefficients of spudcan foundations in stiff-over-soft clay with different shear modulus ratios G_{bs}/G_t.

of shear strain gradually expands, and the energy consumed by soil deformation also increases, thereby gradually increasing the spudcan elastic stiffness, which stabilizes after leaving the influence of the soil surface boundary.

Similarly to the influence of the layered interface (see Section 4.1.1), the moment deformation mechanism has the smallest distribution in the depth direction (see Fig. 9), so the moment elastic stiffness coefficients quickly leave the influence zone of the surface boundary and enter the stabilization zone after the spudcan enters through the soil surface, while the vertical elastic stiffness has not yet stabilized at a depth of 7D (see Fig. 8).

4.1.3. Coupling effect

In practical engineering, the spudcan operating in stiff-over-soft clay is affected by the soil surface boundary and layered interface coupling. This section analyzes these coupling effects. The normalized stiff soil layer thickness t/D was taken as the maximum value reported in practical engineering, which is 2; the shear modulus ratio $G_{bs}/G_t = 0.5$; and the soil heterogeneity coefficients $kD/s_{ubs} = 0,\ 1$ to cover common soil profiles in practical engineering (group IV, Table 1).

As shown in Fig. 10, the elastic stiffness coefficient of the spudcan exhibits a change trend similar to that of "punch-through" failure when the spudcan gradually enters from the soil surface to cross the layered interface into the bottom soft soil. Meanwhile, the phenomenon of "punch-through" failure of vertical elastic stiffness is the least pronounced (Fig. 10), which is similar to the mechanism where a skirted spudcan transfers soil flow to the bottom soft clay by trapping the spudcan base soil, thus mitigating the "punch-through" failure [11,16].

As the vertical deformation mechanism is more widely distributed in the depth direction, it can sense the influence of the layered

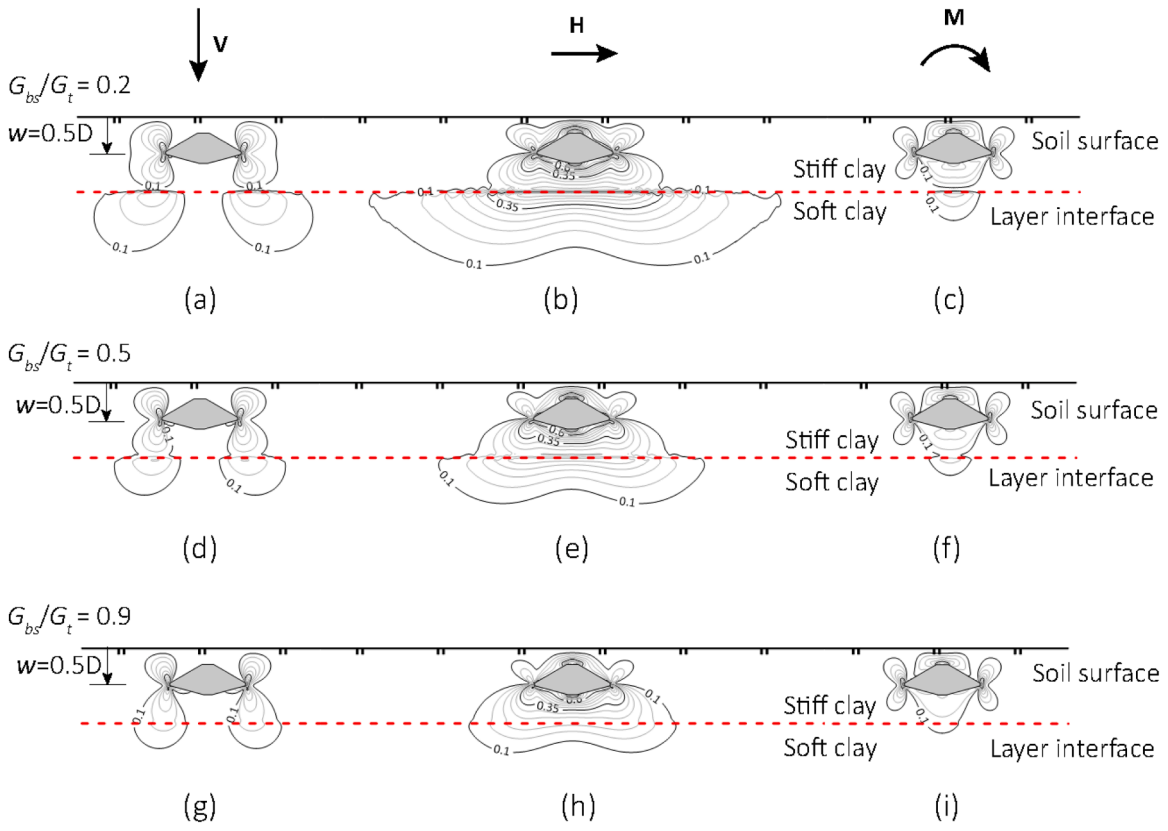

Fig. 14. Shear strain distribution of spudcan foundations in stiff-over-soft clay with different shear modulus ratios G_{bs}/G_t.

interface earlier, allowing soil deformation to spread earlier in the bottom soft clay (see Fig. 11). This, in turn, reduces the effective thickness of the top stiff clay and mitigates the failure risk related to stiffness.

It is further observed from Fig. 10 that there is no longer a stability zone between the soil surface boundary and the soil layered interface. Under the coupling effect of the surface boundary and layered interface, the stability zone between them is "swallowed" or offset by each other (see Fig. 5(d)), which is manifested as the curve of the elastic stiffness coefficient in the top soft soil layer exhibiting an inflection point. Moreover, the influence zone below the layered interface is also weakened to a certain extent, meaning that the spudcan elastic stiffness quickly enters the stability zone after crossing the layered interface. There is no situation in which the elastic stiffness coefficient of the spudcan has not yet entered the stability zone at a depth of 4D in the bottom soft clay, as shown in Section 4.1.1 (see Fig. 4). Note: For bottom soft soil with $k > 0$ (or $kD/s_{ubs} > 0$), the stabilization zone is considered to be reached when the slope of the elastic stiffness coefficient curve is constant (see Fig. 10(b)).

It is worth mentioning that, ideally, when the thickness of the top stiff clay is sufficiently large, there should also be a stability zone between the influence zone of the soil surface boundary and the soil layered interface (see Fig. 5(c)). When the spudcan is in this stability zone, it will be outside the zones of influence of both the surface boundary and the layered interface. However, in practical stiff-over-soft clay profiles, the thickness of the top stiff clay layer is not sufficient to support the occurrence of an intermediate stability zone [13,14]. Therefore, the change in the elastic stiffness coefficient of the spudcan and the corresponding distribution of the influence zone in practical engineering would present the situation depicted in Fig. 5(d).

4.2. *Parametric investigations*

Since the elastic stiffness coefficient curve of spudcan in the above subsection may only apply to a specific combination of thickness ratio t/D, modulus ratio G_{bs}/G_t, and soil heterogeneity coefficient kD/s_{ubs}, this section conducts comprehensive parametric studies on the critical parameters for the safe design of spudcans in stiff-over-soft clay (groups V-VII, Table 1) to expand the current database and promote the development of new design methods. Note: In this section, the spudcan embedment depth is normalized to show more consistent results, and the normalized embedment depth is $\overline{w} = (t - w)/D$. It is worth mentioning that this section adopts the dimensionless approach from Section 4.1 to clearly illustrate the influence of different factors on elastic stiffness. Specifically, a constant shear modulus G_{bs} is used to non-dimensionalize the elastic stiffness into the elastic stiffness coefficient.

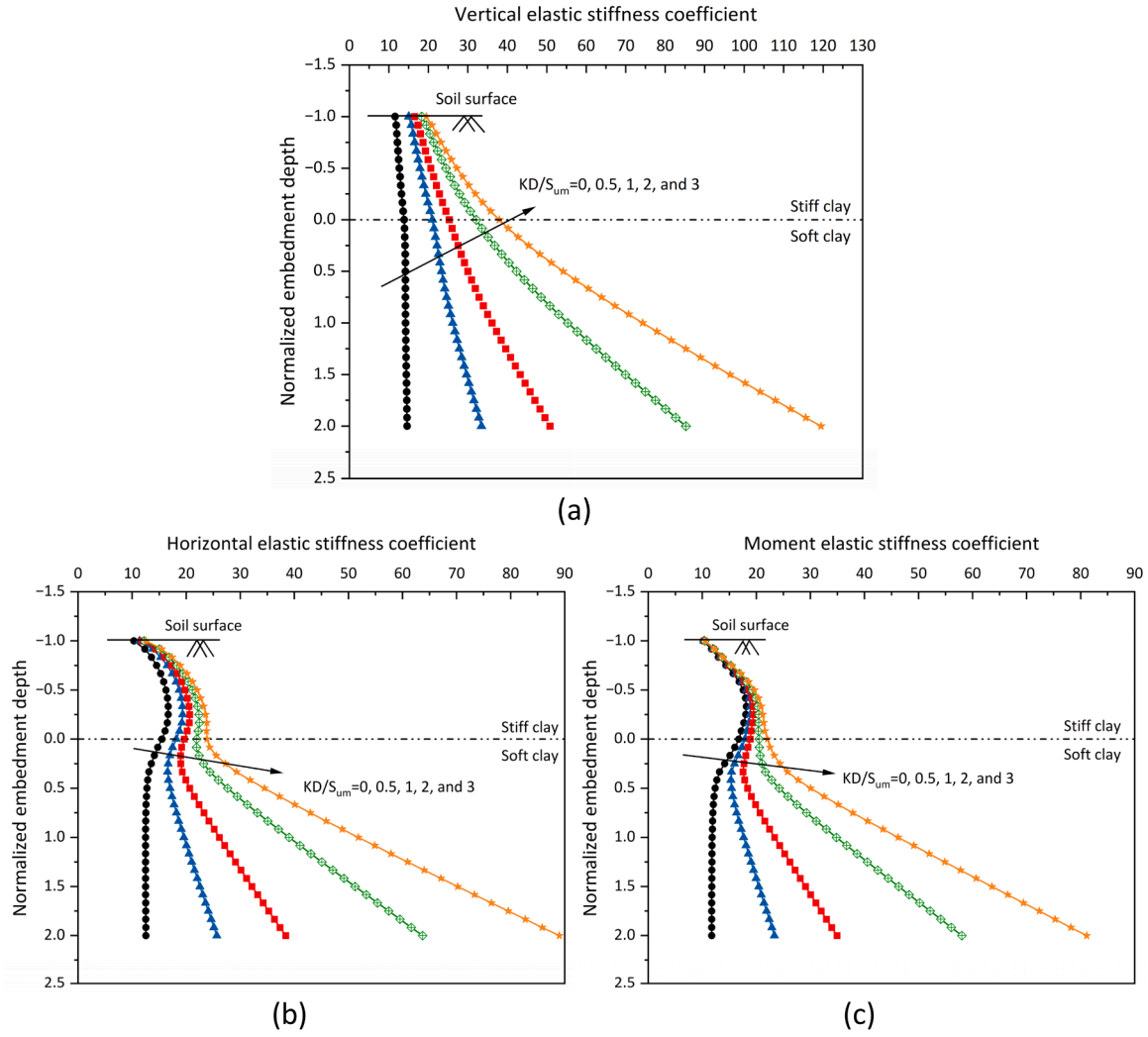

Fig. 15. Elastic stiffness coefficients of spudcan foundations in stiff-over-soft clay with different soil heterogeneous coefficient kD/s_{ubs}.

4.2.1. *Effect of thickness ratio*

As shown in Fig. 12, as the thickness ratio of the top stiff clay t/D increases, the elastic stiffness coefficient curve changes more significantly during the spudcan across the layered interface, and the risk of "punch-through" failure further increases. This is mainly due to the increase in t/D, which increases the embedment depth when the spudcan senses the influence of the layered interface. At this point, the elastic stiffness coefficient of the spudcan is gradually weakened by the influence of the surface boundary and enhanced by the influence of the layered interface. The former increases the spudcan elastic stiffness, while the latter decreases the spudcan elastic stiffness, and the changing trend of spudcan elastic stiffness becomes steep and sharp when the spudcan senses the layered interface.

Also, as mentioned in Section 4.1.3, the vertical elastic stiffness is less affected by t/D because the vertical deformation mechanism is widely distributed in the depth direction. Compared with the horizontal and moment elastic stiffness, the vertical elastic stiffness does not exhibit a significant phenomenon similar to "punch-through" failure (see Fig. 12). The same phenomenon and conclusion can be found in Sections 4.2.2 and 4.2.3, so they are not repeated in the corresponding sections.

Interestingly, the sensitivity of the three directional elastic stiffness coefficients to the influence of soil surface boundary and soil layered interface is also inconsistent. As shown in Fig. 12(a) and (c), the vertical elastic stiffness and moment elastic stiffness enter the stabilization zone after the spudcan crosses the soil surface. There is no influence zone of the surface boundary. In contrast, the horizontal elastic stiffness transitions from the influence zone of the surface boundary to the influence zone of the layered interface. There is no stability zone. The same phenomenon occurs at different shear modulus ratios G_{bs}/G_t and soil heterogeneity coefficient kD/s_{ubs} (see Figs. 13 and 15).

4.2.2. *Effect of shear modulus ratio*

Similar to the effect of t/D, the decrease in the shear modulus ratio G_{bs}/G_t makes the spudcan elastic stiffness more influenced by

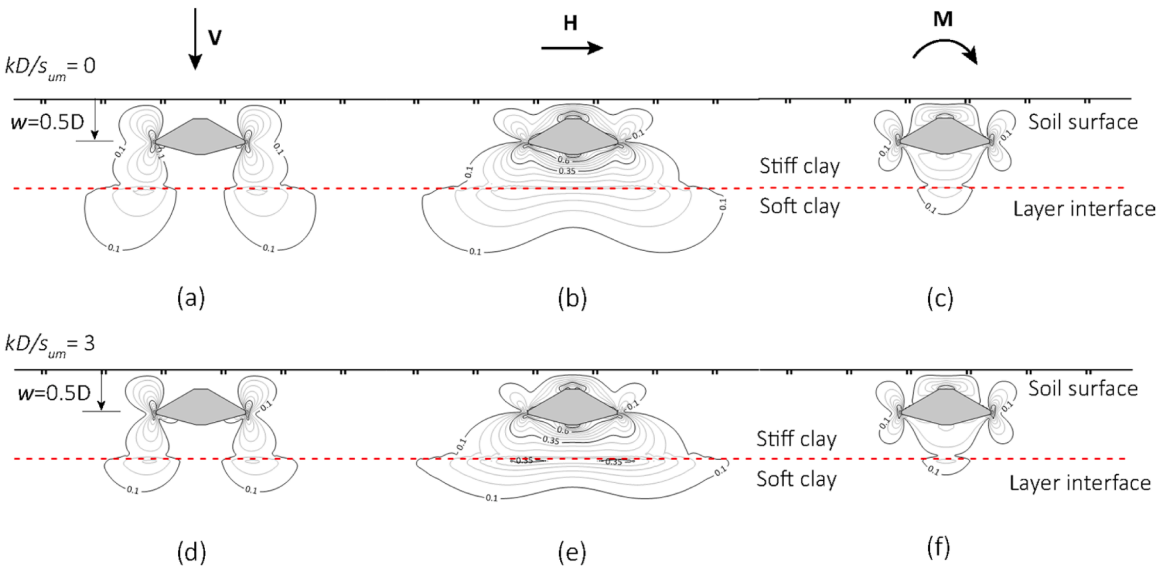

Fig. 16. Shear strain distribution of spudcan foundations in stiff-over-soft clay with different soil heterogeneous coefficient kD/s_{ubs}.

the layered interface. The changing trend of elastic stiffness becomes steeper and sharper during spducan across the layered interface (Fig. 13). The risk of "punch-through" failure also increases with the decrease of G_{bs}/G_t. This is mainly because although the thickness of the top stiff clay does not change, the reduction of the G_{bs}/G_t increases the difference in strength or energy consumption of soil deformation between the layered interfaces, resulting in a more significant change of the spudcan elastic stiffness during spudcan across the layered interface.

Interestingly, the suggestion in Section 4.1.3 that the vertical deformation mechanism of the spudcan is more widely distributed in the depth direction and thus senses the effects of the layered interface earlier and is thus less affected by the layered interface, but this conclusion does not seem to apply to the analysis of different soil properties. As shown in Fig. 14, at the same spudcan embedment depth, the distribution range of shear strain in the bottom soft clay gradually increases as G_{bs}/G_t decreases, but this does not weaken the change gradient of elastic stiffness coefficient of spudcans. In other words, although the increased differences in strength between the layered interfaces caused the spudcan to sense the layered interfaces earlier, this advance prediction has little effect on the drastic change of elastic stiffness caused by the significant difference in strength between soil layer interfaces. i.e., the explanation that wider soil deformation or soil flow mitigates the risk of "punch-through" failure applies only to different foundation shapes [11,16] or different loading directions and does not apply to different soil properties.

4.2.3. *Effect of soil heterogeneity*

As shown in Fig. 15, with the increase of soil heterogeneity coefficient of the bottom soft clay kD/s_{ubs}, the change of elastic stiffness coefficient of the spudcan tends to flatter during the spudcan across the layered interface, which weakens or inhibits the risk of "punch-through" failure to some extent. This is because although the strength difference at the layered interface does not change, the increase of the strength gradient of the bottom soft clay causes the soil strength of the bottom soft clay to increase rapidly with depth so that the difference in the soil strength in a certain range before and after the layered interface is greatly reduced, which makes the spudcan elastic stiffness not to be drastically reduced by sensing the influence of the soil layered interface anymore, i.e., the influence of the layered interface is suppressed.

At the same time, with the increase of kD/s_{ubs}, the spread range of soil deformation to the bottom soft clay decreases (Fig. 16), which indicates that the spreading range of soil deformation does not only depend on the strength difference between the layered interfaces, but is also affected by the soil within a certain range of the layered interfaces. In addition, as shown in Fig. 16, the shear strain of spudcan has an extensive distribution range when kD/s_{ubs} is small, and the risk of "punch-through" failure is precisely the most serious at this time. This also confirms the view in Section 4.2.2 that the explanation that transferring more soil deformation or soil flow to the bottom soft clay mitigates the risk of "punch-through" failure does not apply to the different soil properties analyzed.

It is worth mentioning that although the increase of kD/s_{ubs} suppresses the risk of traditional "punch-through" failure of spudcan elastic stiffness, the excessive kD/s_{ubs} still leads to a sharp increase of spudcan elastic stiffness after spudcan across the layered interface (Fig. 15), which is still a challenge for the safe and stable operation of the spudcan in practical engineering.

4.2.4. *Effect of soil backflow*

Due to the constraint effect of soil backflow filling into the upper cavity of the spudcan, the elastic stiffness coefficient under complete backflow case is greater than that under no backflow case [25]. Obviously, this effect still exists in stiff-over-soft clay. As shown in Fig. 17, as the spudcan crosses the layered interface from the surface and enters the bottom soft clay, the elastic stiffness

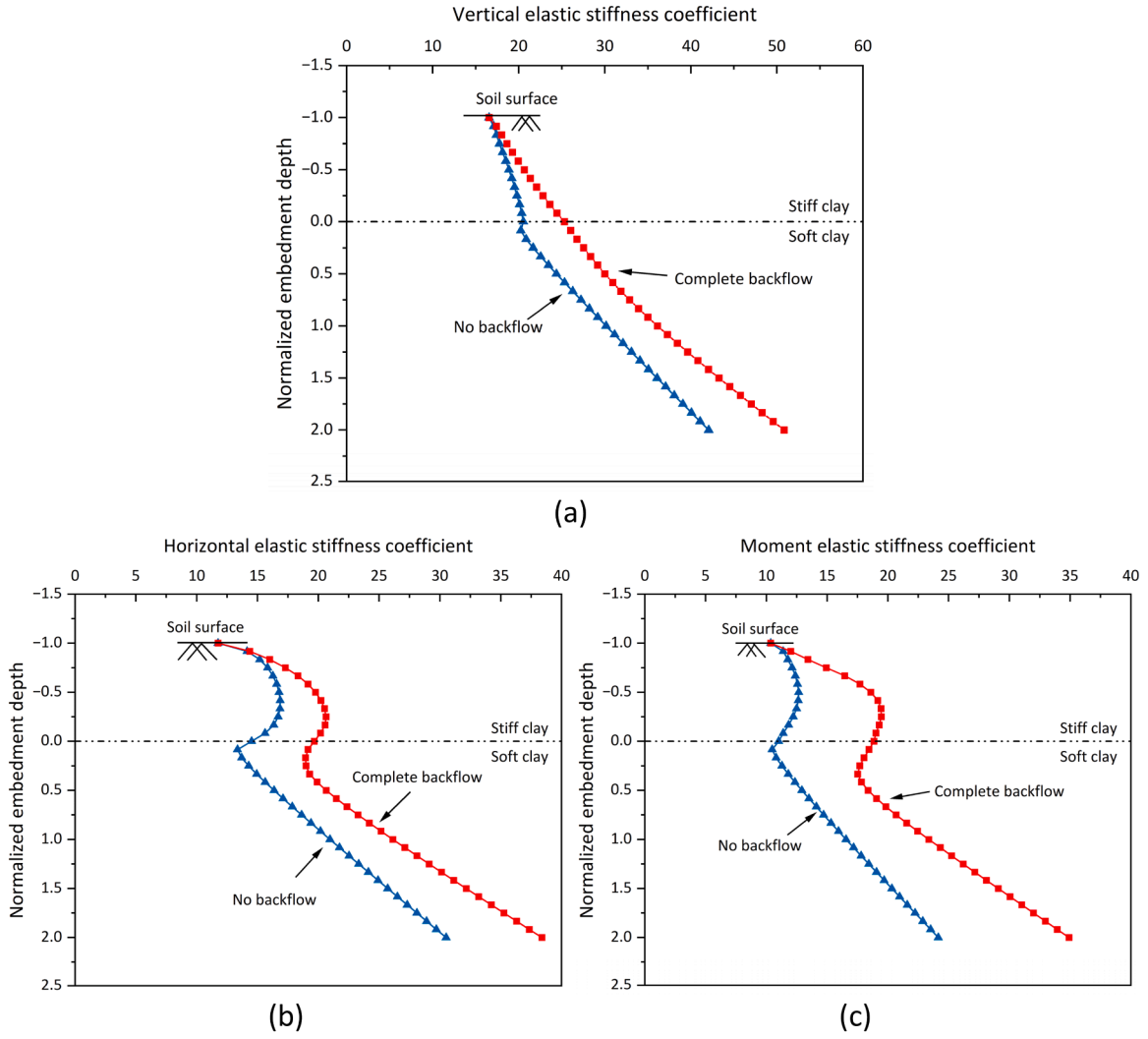

Fig. 17. Elastic stiffness coefficients of spudcan foundations in stiff-over-soft clay with different soil backflow conditions.

coefficient in the no backflow case remains consistently smaller than that in the complete backflow case. However, the change in elastic stiffness coefficient under complete backflow cases exhibits a more dangerous "punch-through" failure phenomenon. This is because the absence of the upper backflow soil weakens the influence of the layered interface. After crossing the layered interface into the bottom soft clay, the spudcans immediately enter the stability zone, forming an elastic stiffness change effect similar to that of single-layer clay.

As shown in Fig. 18, the appearance of cavities above the spudcan (i.e., no backflow case) not only inhibited the development of shear strain around the holes but also reduced the range of shear strain spreading to the bottom soft clay, i.e., inhibited the transfer of soil deformation to the lower soft soil layer. In the complete backflow case, the wider transfer of soil deformation into the bottom soft clay should have sensed the effects of the layered interface earlier. However, it results in a more significant "punch-through" failure phenomenon, which confirms the viewpoint in Section 4.2.

5. Predicted elastic stiffness coefficient profile

As shown in Section 4.2, the variation trends of the elastic stiffness coefficient in different directions do not exhibit consistent patterns. Therefore, to present a uniform or similar variation trend for the elastic stiffness coefficient profile, this section selects G_0 (see Eq. (2)) as the shear modulus in the elastic stiffness matrix (Eq. (1)). As illustrated in Fig. 19, after non-dimensionalizing the elastic stiffness using G_0, the elastic stiffness coefficients in all three directions display similar variation trends: starting from the soil surface, the elastic stiffness coefficient gradually increases, reaches a peak when the spudcan approaches or is located at the soil layer interface, and then gradually converges to a stable value after the spudcan enters the bottom soft clay layer.

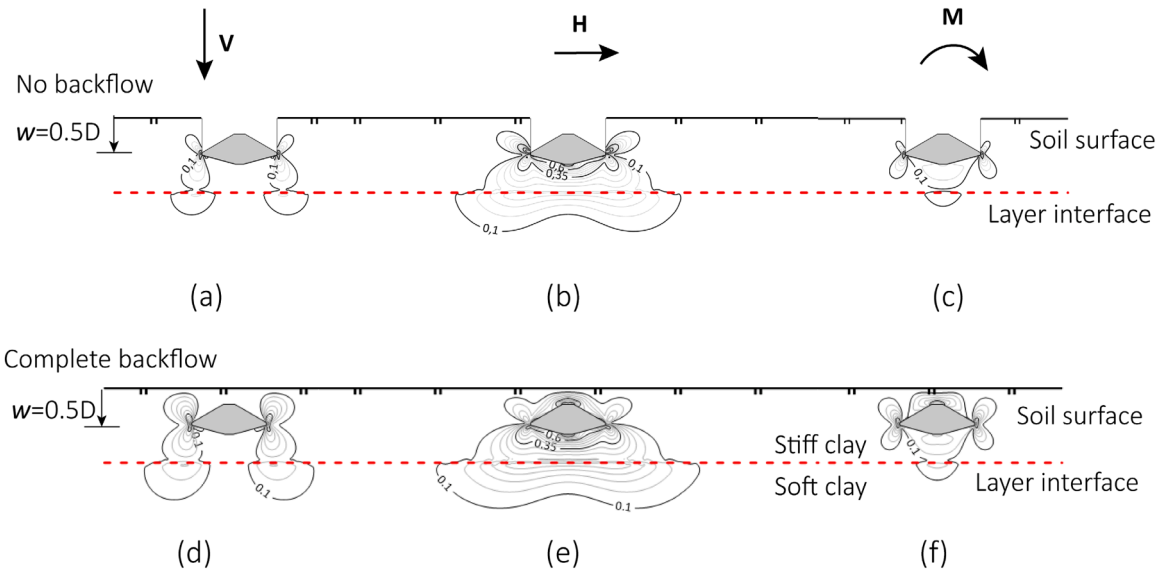

Fig. 18. Shear strain distribution of spudcan foundations in stiff-over-soft clay with different soil backflow conditions.

$$G_0 = \begin{cases} G_{bs}, & 0 < w \le t \\ G_{b0}, & w > t \end{cases} \tag{2}$$

Where G_{b0} is the shear modulus of the bottom soft clay at depth z.

Based on the variation trends of the elastic stiffness coefficients shown in Fig. 19, this section proposes a simplified design profile to predict the changes in the spudcan elastic stiffness coefficient in stiff-over-soft clay (see Fig. 20): (a) determine the elastic stiffness coefficient of the spudcan at the soil surface; (b) determine the elastic stiffness coefficient of the spudcan at the soil layer interface; and (c) determine the elastic stiffness coefficient when the spudcan is located in the stable zone of the bottom soft clay, using this value to approximate the variation of the spudcan elastic stiffness coefficient in the bottom soft clay. Therefore, the three linear segments shown in Fig. 20 can be used to approximately represent the variation profile of the spudcan elastic stiffness coefficient in stiff-over-soft clay. The specific prediction or calculation method is as follows:

(a) soil surface and layered interface location

To comprehensively consider the changes in the elastic stiffness coefficient at the soil surface and the layered interface, an additional 25 sets of orthogonal experiments with different parameter combinations were conducted to cover the parameter range discussed in this study (groups IX, Table 1). After repeated trial calculations, Eq. (3) was proposed to predict the elastic stiffness coefficients in three directions at different soil interfaces. As shown in Fig. 21, Eq. (3) can account for the effects of the thickness ratio t/D, shear modulus ratio G_{bs}/G_t, and soil heterogeneity coefficient kD/s_{ubs}, and the calculated elastic stiffness coefficients show a high level of consistency with the measurement results from numerical simulations. The fitting parameters (i.e., ε_1 - ε_5) in Eq. (3), obtained using the nonlinear least squares method, are listed in Table 2.

$$K_i = \varepsilon_1 + \varepsilon_2 \left(\frac{t}{D}\right)^{\varepsilon_3} \left(\frac{G_{bs}}{G_t}\right)^{\varepsilon_4} \left(\frac{kD}{s_{ubs}} + 1\right)^{\varepsilon_5} \tag{3}$$

Where the subscript i refers to the vertical (V), horizontal (H), and moment (M) directions.

(b) soft clay stability zone

As shown in Fig. 20, after selecting G_0 for non-dimensionalizing the elastic stiffness, the elastic stiffness coefficients of the spudcan in the bottom soft clay under different parameter conditions gradually converge to the same value or fall within a narrow band (Fig. 19). Therefore, this section does not fit the elastic stiffness coefficients of the stable zone in the bottom soft clay under different parameter conditions; instead, it provides the range of variation and the average value (see Table 2) to simplify the prediction process.

6. Recommendation of application in industry practice

Current industry guidelines for jack-up platforms, including SNAME [7] and ISO [15], emphasize that a reasonably accurate assessment of spudcan elastic stiffness is a crucial factor influencing the safe and stable operation of a jack-up platform. However, these

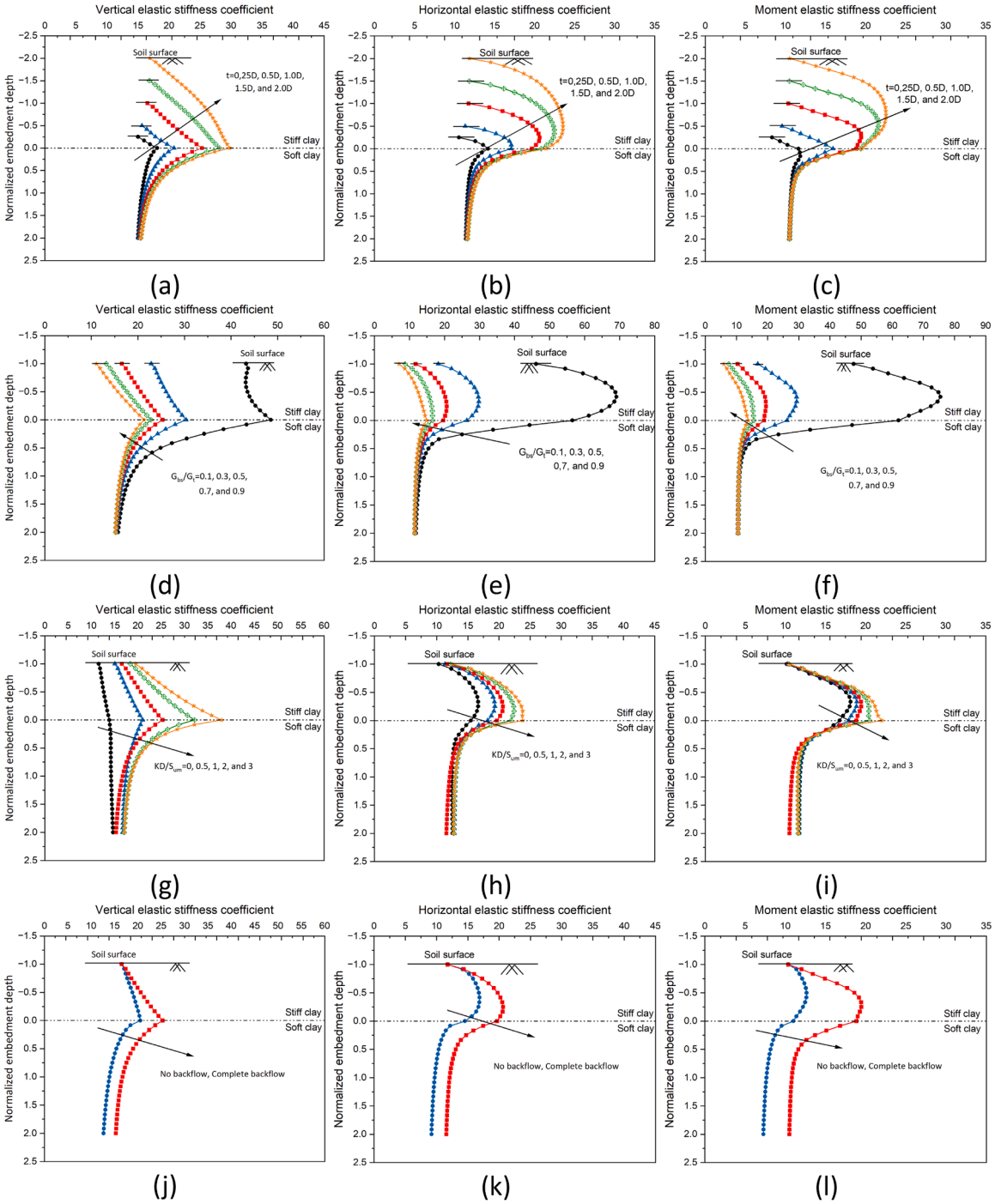

Fig. 19. Elastic stiffness coefficient of the spudcan after non-dimensionalization using G_0.

guidelines primarily address a single-layer, homogeneous soil scenario (i.e., the scenario discussed in Section 4.1.2). The only study on elastic stiffness in layered soils [22] does not consider the effect of the layered interface of the soil, as the spudcan is only positioned in the topsoil, and only a quantitative analysis is available; the corresponding mechanism remains unclear. In this context, this study offers insights for the accurate field assessment of spudcan foundations operating in stiff-over-soft clays.

The results show that: (a) the spudcan elastic stiffness exhibits a changing trend similar to the "punch-through" failure of spudcan penetration resistance in stiff-over-soft clay; (b) the spudcan elastic stiffness in single-layer clay is significantly different from that in layered clay, making it extremely unreasonable and dangerous to use the elastic stiffness value of single-layer clay to evaluate the

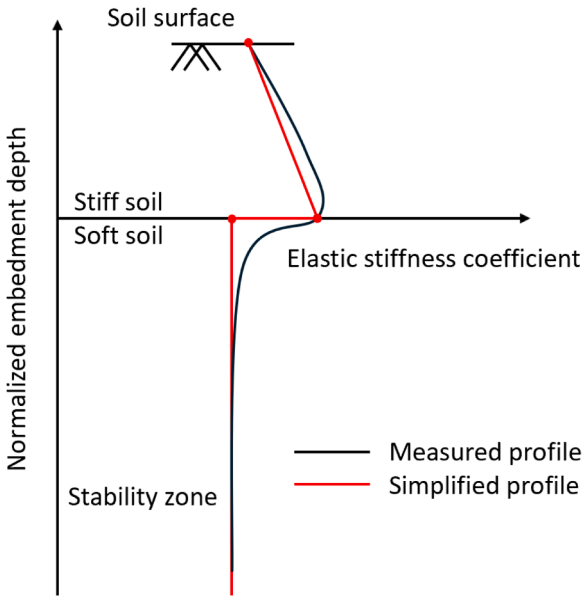

Fig. 20. Schematic diagram of the simplified spudcan elastic stiffness coefficient profile in stiff-over-soft clay.

stiffness changes in layered clay; (c) emphasis should be placed on changes in moment elastic stiffness, which is the most sensitive to soil stratification; (d) for the elastic stiffness coefficient prediction method proposed in this study, its practical application steps are as follows:

1. Obtain soil stratification properties through offshore site investigation and laboratory testing, including G_t, G_{bs}, s_{ubs}, k, t, etc.
2. Calculate the corresponding dimensionless parameters, including t/D, G_{bs}/G_t, kD/s_{ubs}, G_0, etc.
3. Calculate the elastic stiffness coefficients for the no backflow case and the complete backflow case using Eq. (3) and Table 2.
4. Based on the previous steps, the upper and lower bounds of the elastic stiffness of the spudcan in stiff-over-soft clay can be determined. By performing appropriate interpolation based on the embedment depth and backflow condition, a specific value of elastic stiffness can be further estimated.

7. Conclusion remarks

This study discretely simulates the variation in the embedded position of the spudcan in stiff-over-soft clay (similar to the penetration process) using the three-dimensional small-strain finite element (SSFE) method and obtains the complete profile of the spudcan elastic stiffness in stiff-over-soft clay. It isolates and separately evaluates the effects and corresponding mechanisms of the soil surface boundary, the soil layered interface, and the coupling effects between them. A comprehensive parametric study is then carried out to extensively investigate the effect and mechanism of soil stratification on elastic stiffness. The main findings and conclusions are summarized as follows:

(a) The effects of the soil surface boundary and the soil layered interface are competitive rather than mutually promoting, and the two have different effects on elastic stiffness in the three directions.
(b) The vertical deformation mechanism of the spudcan is more widely distributed in the depth direction, allowing for earlier sensing of the effects of the layered interface and resulting in a lower risk of “punch-through” failure.
(c) The increase in soil heterogeneity in the bottom soft clay contributes to mitigating the risk of punch-through failure of elastic stiffness.
(d) This study provides a complete view of the elastic stiffness in stiff-over-soft clays and establishes a simple prediction framework to delineate the effects of the surface boundary and layered interface, which contributes to a more accurate site assessment of jack-up platforms on stiff-over-soft clay sites in complex offshore environments.

CRediT authorship contribution statement

Xiu Zhe Wang: Writing – review & editing, Writing – original draft, Visualization, Validation, Software, Methodology, Investigation, Data curation, Conceptualization. **Xin Tong Wang:** Writing – review & editing, Funding acquisition, Data curation. **Zhen Wang:** Writing – review & editing, Software, Conceptualization. **Fei Liu:** Writing – review & editing, Software. **Qiang Qiang Gao:** Writing – review & editing, Visualization. **Jiang Tao Yi:** Writing – review & editing, Supervision, Resources, Methodology, Funding

profile in stiff-over-soft clay.

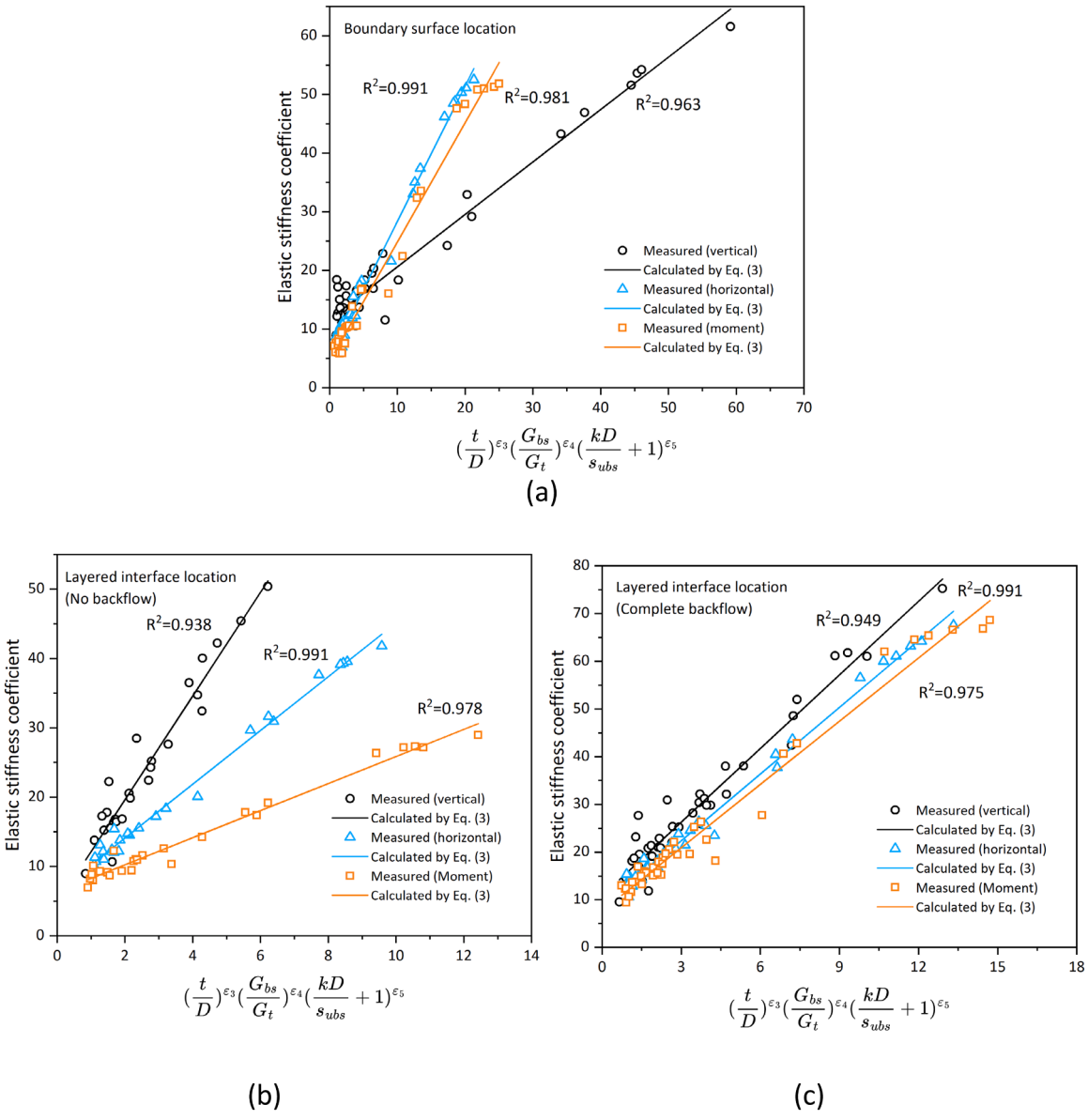

Fig. 21. Comparison of numerical measured results and calculated elastic stiffness coefficients.

Table 2
Summary of fitting parameters and elastic stiffness coefficient of stability zone.

Soil surface location					
	ε_1	ε_2	ε_3	ε_4	ε_5
V	11.668	0.894	0.702	−1.337	0.653
H	5.256	2.309	0.340	−1.163	0.221
M	4.516	2.034	0.478	−1.227	0.155

Layered Interface location (No backflow)						Layered Interface location (Complete backflow)				
	ε_1	ε_2	ε_3	ε_4	ε_5	ε_1	ε_2	ε_3	ε_4	ε_5
V	4.681	7.481	0.334	−0.413	0.675	10.830	5.146	0.619	−0.618	0.804
H	6.372	3.875	0.276	−0.784	0.311	8.385	4.661	0.440	−0.894	0.321
M	6.341	1.953	0.481	−0.819	0.400	7.641	4.424	0.534	−0.955	0.248

Soft clay stability zone (No backflow)	Soft clay stability zone (Complete backflow)
K_V 10.534 – 12.312 (11.934)	15.014 - 17.068 (15.657)
K_H 8.670 – 9.342 (9.012)	11.426 - 12.820 (11.928)
K_M 8.587 – 9.301 (8.879)	10.501 - 11.739 (10.864)

acquisition.

Declaration of competing interest

The authors declare that they have no known competing financial interests or personal relationships that could have appeared to influence the work reported in this paper.

Acknowledgments

The authors wish to acknowledge the National Natural Science Foundation of China (52371259, 52221002, 42307231), and the Natural Science Foundation of Jiangsu Province (BK20220987).

Data availability

Data will be made available on request.

References

[1] Bell R. MSc thesis. University of Oxford; 1991.
[2] Cassidy MJ, Taylor PH, Eatock Taylor R, Houlsby GT. Evaluation of long- term extreme response statistics of jack-up platforms. Ocean Eng 2002;29(13):1603–31. https://doi.org/10.1016/S0029-8018(01)00110-X.
[3] Cassidy MJ, Vlahos G, Hodder M. Assessing appropriate stiffness levels for spudcan foundations on dense sand. Mar struct 2010;23(2):187–208. https://doi.org/10.1016/j.marstruc.2010.03.003.
[4] Cheng P, Liu F, Chen X, Zhang Y, Yao K. Estimation of the installation torque–capacity correlation of helical pile considering spatially variable clays. Can Geotech J 2024;61(10):2064–74. https://doi.org/10.1139/cgj-2023-0331.
[5] Cotterill CJ, Phillips E, James L, Forsberg CF, Tjelta TI, Carter G, Dove D. The evolution of the Dogger Bank, North Sea: a complex history of terrestrial, glacial and marine environmental change. Quat Sci Rev 2017;171:136–53. https://doi.org/10.1016/j.quascirev.2017.07.006.
[6] Dassault Systèmes. Abaqus users' manual, version 6.14. Providence, RI, USA: Simulia Corp; 2014.
[7] Society of Naval Architects and Marine Engineers. Site specific assessment of mobile jack-up units. Jersey City, NJ: SNAME; 2008.
[8] Poulos HG. Marine geotechnics. London: Unwin Hyman; 1988.
[9] Purwana OA, Leung C, Chow Y, Foo K. Influence of base suction on extraction of jack-up spudcans. Géotechnique 2005;55(10):741–53. https://doi.org/10.1680/geot.2005.55.10.741.
[10] Hambly EC, IMM GR, Stahl B. Jack-up performance and foundation fixity under developing storm conditions. In: Offshore Technology Conference; 1990.
[11] Hossain MS, Hu Y, Ekaputra D. Skirted foundation to mitigate spudcan punchthrough on sand-over-clay. Géotechnique 2014;64(4):333–40. https://doi.org/10.1680/geot.13.T.027.
[12] Hossain MS, Hu Y, Randolph MF, White DJ. Limiting cavity depth for spudcan foundations penetrating clay. Géotechnique 2005;55(9):679–90. https://doi.org/10.1680/geot.2005.55.9.679.
[13] Hossain MS, Randolph MF. Deep-penetrating spudcan foundations on layered clays: centrifuge tests. Géotechnique 2010;60(3):157–70. https://doi.org/10.1680/geot.8.P.039.
[14] Hossain MS, Randolph MF. Deep-penetrating spudcan foundations on layered clays: numerical analysis. Géotechnique 2010;60(3):171–84. https://doi.org/10.1680/geot.8.P.040.
[15] ISO/FDIS. Petroleum and natural gas industries—site-specific assessment of mobile offshore units— part 1: jack-ups. Geneva: ISO; 2016.
[16] Li YP, Liu Y, Lee FH, Goh SH, Zhang XY, Wu J-F. Effect of sleeves and skirts on mitigating spudcan punch-through in sand overlying normally consolidated clay. Géotechnique 2019;69(4):283–96. https://doi.org/10.1680/jgeot.17.P.085.
[17] Lin W-L, Wang Z, Liu F, Yi J-T. The effects of installation on the elastic stiffness coefficients of spudcan foundations. J Mar Sci Eng 2021;9(4):429. https://doi.org/10.3390/jmse9040429.
[18] Liu F, Cheng P, Luo YJ, Yi JT, Chen XJ, Peng Y, Chu YP. Large-deformation study of T-bar penetration in spatially variable sediments. Appl Ocean Res 2024;150:104105. https://doi.org/10.1016/j.apor.2024.104105.
[19] Liu F, Cheng P, Wang Z, Yi JT, Chen XJ, Peng Y, Hu J. Effect of soil spatial variability on the stability of pipelines under horizontal loading. Comput Geotech 2024;175:106671. https://doi.org/10.1016/j.compgeo.2024.106671.

[20] Wang XZ, Yi JT, Sun MJ, Liu F, Xu SJ. Determination of elastic stiffness coefficients for spudcan foundations in a spatially varying clayey seabed. Appl Ocean Res 2022;128:103336. https://doi.org/10.1016/j.apor.2022.103336.
[21] Wang XZ, Yi JT, Sun MJ, Xie Q, Pan YT. Time evolution of elastic stiffness coefficients for a jack-up spudcan in clay during operation. Comput Geotech 2023; 154:105181. https://doi.org/10.1016/j.compgeo.2022.105181.
[22] Wang Y, Cassidy MJ, Bienen B. Elastic stiffness of circular footings on clay overlying sand under general loading. Geotech. Lett. 2020;10(4):498–509. https://doi.org/10.1680/jgele.20.00045.
[23] Yi JT, Huang LY, Li DQ, Liu Y. A large-deformation random finite-element study: failure mechanism and bearing capacity of spudcan in a spatially varying clayey seabed. Géotechnique 2020;70(5):392–405. https://doi.org/10.1680/jgeot.18.P.171.
[24] Yin S, Xiang YZ, Xu J, Cheng H, Jiang YW, Cai GJ, Yi JT. Elastic stiffness coefficients of a skirted spudcan foundation in clay. Appl Ocean Res 2022;120. https://doi.org/10.1016/J.APOR.2022.103054. 103054-103054.
[25] Zhang Y, Cassidy MJ, Bienen B. Elastic stiffness coefficients for an embedded spudcan in clay. Comput Geotech 2012;42:89–97. https://doi.org/10.1016/j.compgeo.2011.12.011.
[26] Zheng J, Hossain MS, Wang D. Prediction of spudcan penetration resistance profile in stiff-over-soft clays. Can Geotech J 2016;53(12):1978–90. https://doi.org/10.1139/cgj-2015-0339.